PAPER

Check for updates

Indirect aqueous carbonation of $CaSO_4 \cdot 2H_2O$ with aspartic acid as a recyclable additive

Yuan Gong, [ID] [ab] Xuechen Zhu,[a] Zhuo Yang,[a] Xin Zhang[a] and Chunlei Li[*ab]

Calcium leaching using additives is the most critical step in the indirect aqueous carbonation process of $CaSO_4 \cdot 2H_2O$. However, recovery of the soluble additives from the sulfate-rich carbonation filtrate limits the large-scale industrial implementation of current carbonation technologies. To address this issue, we employed aspartic acid (Asp) as a leaching additive. The dissolution capability of $CaSO_4 \cdot 2H_2O$ in aqueous ammonia was found to improve significantly owing to the complexation effect between Asp and the Ca^{2+} ions. The maximum amount of dissolved $CaSO_4 \cdot 2H_2O$ was determined according to the competitive relationship between the complexing effect and the inhibitory effect of free ammonia molecules on the dissociation of $CaSO_4 \cdot 2H_2O$, and the solution pH influences such competition. The precipitation of $CaCO_3$ was examined by monitoring the variations in the pH and conductivity of the carbonation reaction system. As a result, the shift in the Asp dissociation equilibrium extended the induction period, and the growth period was divided into three stages according to the relative difference between the consumption and formation rates of CO_3^{2-}. Moreover, it was determined that the carbonation products consisted of stable spherical vaterite particles. The recovery of Asp was also demonstrated at its isoelectric point, with a recovery efficiency of >80% being achieved, and recycling experiments confirmed the stability of the recycled Asp. Finally, the amount of dissolved $CaSO_4 \cdot 2H_2O$ and the total carbonation efficiency during cycling were determined as 16.3 ± 0.4 g L^{-1} and $46.5 \pm 1.9\%$, respectively.

1. Introduction

Aqueous carbonation is a promising approach for CO_2 capture, utilisation, and storage, and this process can be carried out via either a direct or an indirect route.[1] Remarkably, the indirect pathway has received increasing attention in the last two decades because of its mild reaction conditions, high conversion efficiency, and capability to obtain high-purity carbonate products.[2] The large-scale dumping of the industrial byproduct gypsum (BG) in open air, such as phosphogypsum (PG) and flue gas desulfurization gypsum (FGDG), has caused severe environmental pollution and resource wastage.[3] According to chemical analysis, the main component of BG is $CaSO_4 \cdot 2H_2O$ with a theoretical CaO content of 32.5 wt%, which can store about 0.26 kg ton^{-1} of CO_2.[4] Furthermore, the annual output of BG is more than 430 million tons, and thus almost 120 million tons of CO_2 would be converted into $CaCO_3$ by carbonation reaction every year.[4–6] Therefore, the exploration of efficient and economically feasible indirect aqueous carbonation methods based on the use of $CaSO_4 \cdot 2H_2O$ would be expected to promote

the industrial development of the flue gas CO_2 carbonation process using BG. Furthermore, such an approach could synergistically reduce CO_2 emissions and utilise the waste BG.[7]

Conventionally, the indirect aqueous carbonation route using $CaSO_4 \cdot 2H_2O$ mainly involves two successive steps: (a) calcium leaching from $CaSO_4 \cdot 2H_2O$ using additives to obtain a calcium-rich leachate solution, and (b) the precipitation of $CaCO_3$ *via* the gas–liquid carbonation reaction of CO_2 (g) with Ca^{2+} (aq.) after adjusting the above leachate solution to an alkaline pH by the addition of a basic medium.[8] It is well known that the solubility of $CaSO_4 \cdot 2H_2O$ in pure water is extremely low (*i.e.*, 0.26 g per 100 g H_2O at 25 °C). This low solubility limits the yield of $CaCO_3$ during the subsequent gas–liquid carbonation reaction because of the inadequate calcium content in the liquid phase. Therefore, the use of additives in the leaching step is critical for improving the solubility of $CaSO_4 \cdot 2H_2O$ in aqueous media.

Based on the salt and complex effects, researchers have reported several effective leaching additives, such as NaCl,[9] CH_3-$COONH_4$,[10] NH_4Cl,[11] and $NaC_6H_{11}O_7$.[12] However, together with the release of Ca^{2+}, the SO_4^{2-} that is leached from $CaSO_4 \cdot 2H_2O$ can form a byproduct sulfate salt with the cationic component of the added basic medium. Generally, the formed sulfate salt is highly soluble in aqueous solutions and thus difficult to separate from the equally soluble additives mentioned above.

aSchool of Petrochemical Technology, Lanzhou University of Technology, Gansu, Lanzhou 730050, PR China. E-mail: lichunlei33@qq.com

bKey Laboratory of Low Carbon Energy and Chemical Engineering of Gansu Province, Lanzhou University of Technology, Gansu, Lanzhou 730050, PR China
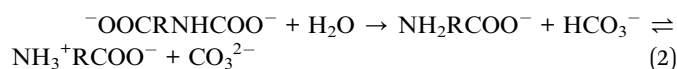
Conversely, if the carbonation filtrate containing the sulfate salt and the additive is recycled directly after removing the $CaCO_3$ precipitate, as previously reported by Chen *et al.*,[9,11] the content of the sulfate salt increases as the filtrate cycle number increases, inhibiting the dissolution of $CaSO_4 \cdot 2H_2O$ due to the common ion effect. These drawbacks therefore limit the recycling and recovery of the leaching additives, which is a significant hurdle in the large-scale industrial implementation of the indirect aqueous carbonation process based on the use of BG.[7]
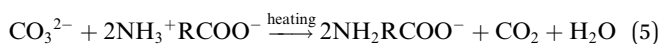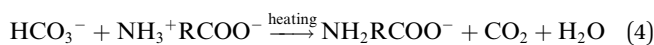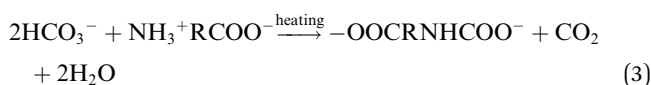
Aspartic acid (Asp) contains both carboxyl (–COOH) and amino (–NH₂) groups in its molecular structure, and so it can form a soluble chelate with Ca^{2+} under alkaline conditions.[13] Based on this complexation effect, we previously demonstrated that the use of Asp as a leaching additive can significantly improve the dissolution capability of $CaSO_4 \cdot 2H_2O$ in aqueous ammonia. Moreover, as an amphoteric electrolyte, the solubility of Asp in aqueous solutions is closely related to the solution pH. More specifically, the minimum solubility of Asp at 25 °C is 0.50 g per 100 g H_2O at its isoelectric point (pI = 2.77),[14] and this solubility increases rapidly upon increasing the solution pH. This unique feature provides a strategy to effectively separate Asp from the sulfate salt-containing carbonation filtrate by simply adjusting the pH value.

Upon reviewing previous works into leaching additives, it was found that other organic compounds containing the –COOH functionality, such as succinic acid, citrate, and EDTA acid, could enhance the degree of calcium leaching. However, because of the strong complexation capability with calcium, carbonate precipitates are not always formed during the carbonation reaction.[15,16] In addition, Song *et al.*[17] found that the addition of polyacrylic acid lowered the overall carbonation yield *via* CO_2 emission, thus reducing the CO_2 dissolution. The chelate formed by some amino acids and Ca^{2+} dissociates with decreasing pH, and $CaCO_3$ precipitates are formed during the dissociation process.[18] Furthermore, the –NH₂ groups of amino acids can react with dissolved CO_2 to promote the absorption of CO_2 gas, wherein the absorption and thermal desorption reaction mechanisms are similar to those of the alkanolamines due to their comparable functional group compositions, and they are given by the following equations:[19,20]

Absorption reaction follows the zwitterion mechanism:

$$2NH_2RCOO^- + CO_2 \rightarrow \underset{\text{carbamate}}{{}^-OOCRNHCOO^-} + \underset{\text{zwitterionic ion}}{NH_3{}^+RCOO^-}$$
(1)

$$^-OOCRNHCOO^- + H_2O \rightarrow NH_2RCOO^- + HCO_3{}^- \rightleftharpoons NH_3{}^+RCOO^- + CO_3{}^{2-}$$
(2)

Thermal desorption reaction:

$$2HCO_3{}^- + NH_3{}^+RCOO^- \xrightarrow{\text{heating}} {}^-OOCRNHCOO^- + CO_2 + 2H_2O$$
(3)

$$HCO_3{}^- + NH_3{}^+RCOO^- \xrightarrow{\text{heating}} NH_2RCOO^- + CO_2 + H_2O$$
(4)

$$CO_3{}^{2-} + 2NH_3{}^+RCOO^- \xrightarrow{\text{heating}} 2NH_2RCOO^- + CO_2 + H_2O$$
(5)

$$^-OOCRNHCOO^- + NH_3{}^+RCOO^- \xrightarrow{\text{heating}} 2NH_2RCOO^- + CO_2$$
(6)

where R represents the side chain (R group) of each amino acid. In this context, Liu *et al.*[21] reported a single-step direct aqueous carbonation method for CaO and $CaSiO_3$, which was based on the use of sodium glycinate. This method adopted the integrated CO_2 absorption and mineralisation (IAM) technology,[22,23] which could reduce the energy consumption of glycinate regeneration through a chemical method instead of the traditional thermal method (*i.e.*, eqn (3)–(6)). According to their study, as shown in eqn (1), the dissolved CO_2 reacts with glycinate to generate the corresponding carbamate and zwitterionic ion. The formation of $CaCO_3$ through carbonation reaction can greatly facilitate carbamate hydrolysis (*i.e.*, eqn (2)) to regenerate glycinate. Simultaneously, the zwitterionic ion can also be converted to glycinate under alkaline conditions. They also found that glycinate can undergo multiple CO_2 capture and regeneration cycles, thereby confirming the feasibility of amino acid regeneration through the carbonation approach. Furthermore, Ji *et al.*[24] recently proposed an indirect aqueous carbonation method coupled with the IAM technology, which was based on the use of protonated amino acids to dispose of alkaline solid waste (the main component being CaO). In this system, the amino acid content ranged from 1 to 2 mol L^{-1}, and the degree of protonation was 20–80%; however, because of the particularity of the calcium source, the only byproduct of the carbonation reaction carried out using CaO was H_2O, which differs from the generation of additional byproduct when $CaSO_4 \cdot 2H_2O$ was employed. Thus, the major drawback associated with the accumulation of sulfate salts during amino acid recycling was ignored in their report.

Thus, we herein propose an indirect aqueous carbonation method of $CaSO_4 \cdot 2H_2O$ with Asp as a recyclable leaching additive. Initially, we examine the dissolution capability of $CaSO_4 \cdot 2H_2O$ in aqueous ammonia in the presence of Asp under different ammonia contents and liquid-to-solid ratios. Subsequently, the precipitation process of $CaCO_3$ from the leachate solution is analysed based on variations in the pH and conductivity, and a detailed transformation mechanism is described for Asp. Moreover, the feasibility of recovering Asp from the carbonation filtrate at its isoelectric point is evaluated by Fourier transform infrared (FTIR) spectroscopy. Finally, the recovery efficiency and further cycle performance of Asp based on the amount of dissolved $CaSO_4 \cdot 2H_2O$ and the total carbonation efficiency are examined over 10 recycling experiments.

2. Experimental

2.1 Materials

As a preliminary study, the current work ignores the influence of the BG impurity on the carbonation reaction. Therefore, analytically pure $CaSO_4 \cdot 2H_2O$ (Sinopharm Chemical Reagent Co., Ltd, China) was selected as the calcium source for carbonation. NH_4OH (AR grade) and H_2SO_4 (AR grade) were purchased from Sinopharm Chemical Reagent Co., Ltd, China.

Asp (levo form, biotech grade) was purchased from Macklin Biochemical Co., Ltd, China. Industry-grade CO_2 with a purity of 99.9% was used for the carbonation reaction. Deionised water supplied by an ultra-pure water system was used to prepare all solutions.

2.2 Methods

2.2.1 Leaching experiments. A series of batch leaching experiments were performed in closed-glass round-bottom flasks. More specifically, Asp (9.66 g) was initially dissolved in aqueous ammonia at different volumes and ammonia contents. Subsequently, $CaSO_4 \cdot 2H_2O$ powder (5 g) was added to the alkaline solution and mixed well by magnetic stirring at 30 °C until the dissolution equilibrium was achieved (*i.e.*, ~60 min). The leaching temperature was selected to avoid the escape of gaseous NH_3, and the molar ratio of Asp to $CaSO_4 \cdot 2H_2O$ was equal to 2.5 to ensure a slight excess of Asp in the leaching systems.[13] Suspensions saturated in calcium were filtered to obtain the Ca-rich leachate solutions. The amount of dissolved $CaSO_4 \cdot 2H_2O$ (η) was measured by complexometric titration using an EDTA standard solution of 0.01 mol L^{-1}. The detailed experimental parameters for the leaching process are listed in Table 1.

2.2.2 Carbonation reaction experiments. A five-necked glass-jacketed reactor with a 500 mL capacity was used for the gas–liquid carbonation reaction. More specifically, $CaSO_4 \cdot 2H_2O$ powder (15 g) was dissolved in a solution with an ammonia content of 7 wt% and a liquid-to-solid ratio of 30. This system was initially chosen considering the ideal $CaSO_4 \cdot 2H_2O$ leaching capability and a higher initial carbonation reaction pH, which is beneficial for $CaCO_3$ formation. At the beginning of the reaction, CO_2 gas was directly injected into the obtained Ca-rich

leachate solution at a rate of 500 mL min^{-1} using a mass flowmeter (SLD-MFC, SENLOD, China). The stirring rate was maintained at 500 rpm using an overhead stirrer (EUROSTAR 20 digital, IKA, Germany). As the carbonation reaction is exothermic, the reaction heat was removed from the reaction system by cooling circulating water, and the reaction temperature was maintained at 30 ± 1 °C. During the 50 min reaction time, the system pH and conductivity were recorded online using a pH meter (PHSJ-6L, INESA, China) and a conductivity meter (DDSJ-319L, INESA, China), respectively. The reactive suspensions were sampled (1 mL) at predetermined time intervals and filtrated using 0.2 μm membrane filters prior to analysis of the dissolved calcium content by titration with EDTA. The amount of precipitated $CaCO_3$ at each time interval was obtained from the difference between the determined content and the initial dissolved calcium content. At the end of the reaction, the final $CaCO_3$ production was recovered *via* filtration and washing with aqueous ammonia of 7 wt%. The sample was then dried to constant weight to determine its mass with gravimetric method. The polymorphs and morphologies of the obtained $CaCO_3$ were characterised by X-ray diffraction (XRD; Ultima IV, Rigaku, Japan, Cu Kα radiation source in a 2θ range of 5–90° at a scanning rate of 1° min^{-1}) and scanning electron microscopy (SEM; Sigma 300, ZEISS, Germany, accelerating voltage of 5 kV). The total carbonation efficiency (γ) was calculated according to the equation, as previously described by Rahmani *et al.*:[25]

$$\gamma(\%) = \frac{m_{Ca,end}}{m_{TCa,initial}} \times 100 \qquad (7)$$

where $m_{Ca,end}$ (g) and $m_{TCa,initial}$ (g) represent the calcium amount of the final $CaCO_3$ products and $CaSO_4 \cdot 2H_2O$ raw material, respectively.

2.2.3 Asp recovery and recycling experiments. After the removal of $CaCO_3$, the filtrate was evaporated at 90 °C under reduced pressure to remove any excess aqueous ammonia. After evaporation, the pH of the filtrate was close to neutral. Subsequently, a 40 wt% H_2SO_4 solution was added at 25 °C to further adjust the pH to the isoelectric point of Asp (*i.e.*, 2.77). The variation in pH during addition of the H_2SO_4 solution was recorded, and the precipitated solid phase obtained at the isoelectric point was filtered and dried in an oven at 100 °C until reaching a constant weight (12 h). The identities of the obtained products were confirmed by means of FTIR spectrometry. In addition, the recovery efficiency of Asp (φ) was determined as follows:

$$\varphi(\%) = \frac{m_{Asp,recovered}}{m_{Asp,leaching}} \times 100 \qquad (8)$$

where $m_{Asp, recovered}$ (g) and $m_{Asp,leaching}$ (g) denote the amount of Asp recovered from carbonation filtrate and added during the leaching step, respectively. Finally, as outlined in Fig. 1, the Asp recycling experiments were performed after supplementing the loss of Asp with the fresh reagent to examine the cycling performance of Asp. It should be noted here that the additional fresh Asp required for each recycle was <20 wt% of the total Asp content.

Table 1 Leaching experimental parameters

No.	Content		L/S ratio (mL g^{-1})	pH[a]
	Asp (mol L^{-1})	Ammonia (wt%)		
1	0.726	3	20	9.472
2	0.484	3	30	9.761
3	0.363	3	40	10.055
4	0.290	3	50	10.102
5	0.726	5	20	9.834
6	0.484	5	30	10.004
7	0.363	5	40	10.263
8	0.290	5	50	10.336
9	0.726	7	20	10.097
10	0.484	7	30	10.266
11	0.363	7	40	10.515
12	0.290	7	50	10.555
13	0.726	9	20	10.208
14	0.484	9	30	10.425
15	0.363	9	40	10.625
16	0.290	9	50	10.677
17	0.726	11	20	10.385
18	0.484	11	30	10.522
19	0.363	11	40	10.734
20	0.290	11	50	10.802

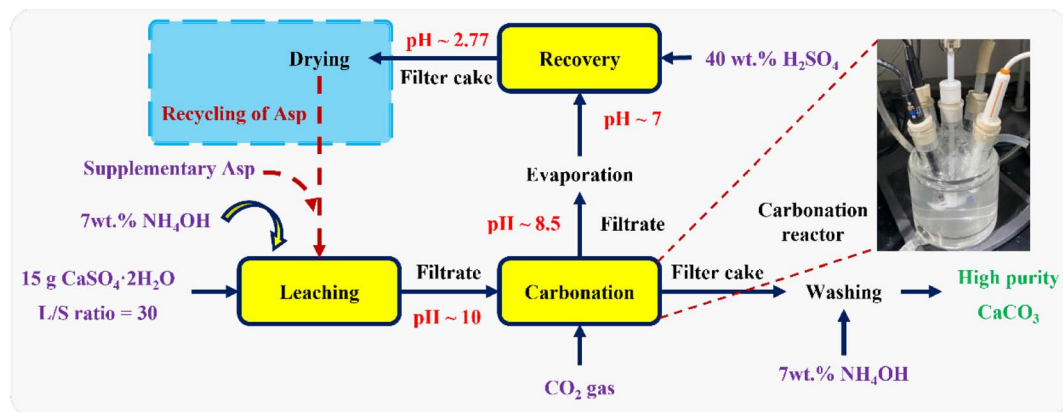[a] pH values were measured under 25 °C.

Fig. 1 Schematic outline of the multistep experimental procedure, including calcium leaching, the carbonation reaction, Asp recovery, and Asp recycling.

3. Results and discussion

3.1 Influence of the ammonia content and liquid-to-solid ratio on calcium leaching in the presence of Asp

As shown in Fig. 2a, compared with the extremely low solubility of $CaSO_4 \cdot 2H_2O$ in aqueous ammonia, the presence of Asp resulted in a significant increase in the amount of dissolved $CaSO_4 \cdot 2H_2O$ (η). Furthermore, upon varying the ammonia content and liquid-to-solid ratio, η was found to exhibit different tendencies. More specifically, at a given ammonia content, the value of η gradually decreased as the liquid-to-solid ratio increased due to the increased activity of H_2O, while the solubility constant of $CaSO_4 \cdot 2H_2O$, which is defined as the product of the activities of Ca^{2+}, SO_4^{2-}, and H_2O, remained unchanged at a given temperature.[26,27] Besides, the complexing effect weakened due to the Asp content decreasing with the increase of the liquid-to-solid ratio. In contrast, the value of η increased upon increasing the ammonia content to 7%, beyond which point, the value of η decreased again. Moreover, it is worth noting that with the exception of a liquid-to-solid ratio of 50, the ammonia content corresponding to the maximum value of η remained constant at 7% (*c.f.*, 5% for a liquid-to-solid ratio of 50) over the various liquid-to-solid ratios examined herein (see Fig. 2a).

According to previous research, the dissolution of $CaSO_4 \cdot 2H_2O$ in aqueous ammonia is inhibited due to the formation of hydrogen bonds between free ammonia molecules and bound water molecules in the layered crystal structure of $CaSO_4 \cdot 2H_2O$,[28] thereby accounting for the later decrease in solubility at higher ammonia contents. More specifically, the observed variation in η appeared to be controlled by competition between the positive complexing effect (Asp with Ca^{2+}) and the negative inhibitory effect (free ammonia molecules with bound water molecules); the former was dominant at relatively low ammonia contents, while the latter played a more significant role at high ammonia contents.

As shown in Fig. 2b, over a given ammonia content range, the mass of Asp remained constant, thereby indicating that the pH of the leachate solution is proportional to the liquid-to-solid ratio. More specifically, upon increasing the liquid-to-solid ratio, a higher pH led to an increase in the free ammonia molecules content, considering the shift in the dissociation
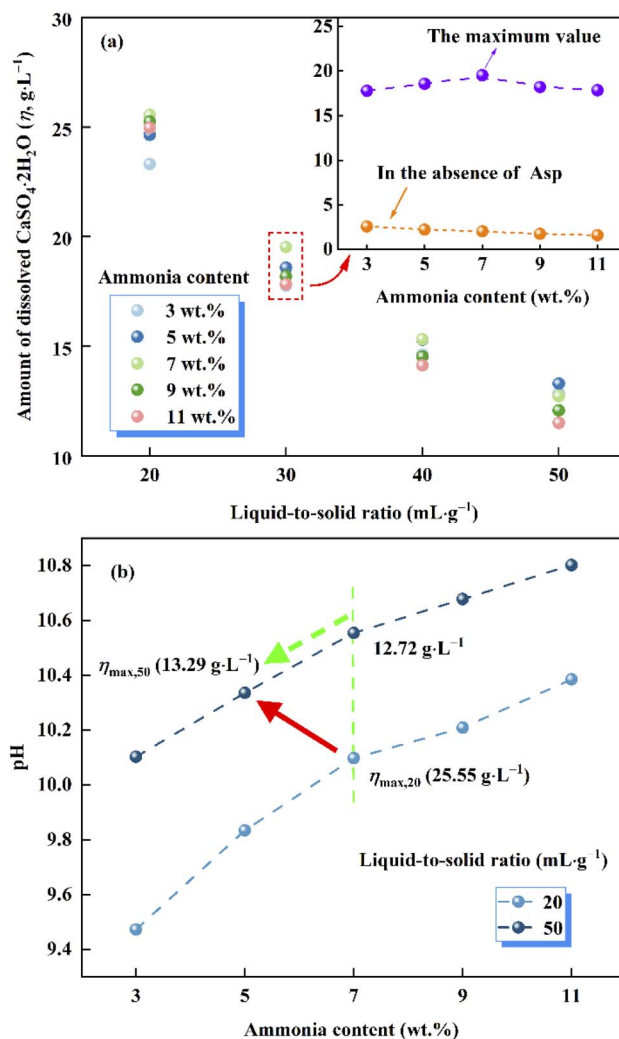

Fig. 2 (a) Plot of the amount of dissolved $CaSO_4 \cdot 2H_2O$ (η) *vs.* the liquid-to-solid ratio and the ammonia content. (b) Plot of the pH *vs.* the ammonia content at liquid-to-solid ratios of 20 and 50.
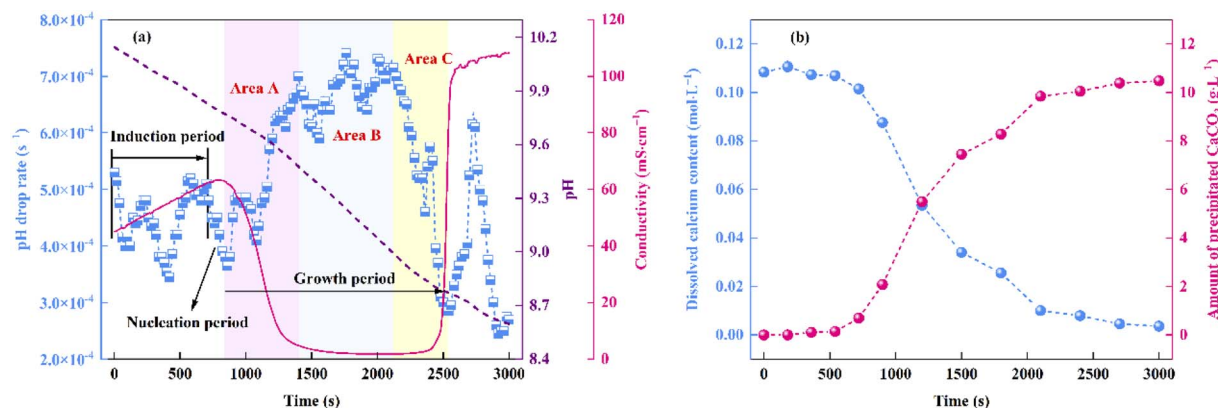
Fig. 3 Variations in the (a) pH and conductivity of the reaction system over time. (b) Contents of dissolved Ca and precipitated $CaCO_3$ during the progress of the carbonation reaction.
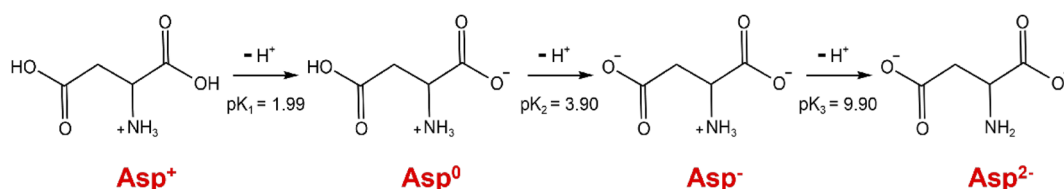

Fig. 4 Dissociation equilibrium shift of Asp.

equilibrium of ammonia. According to the above competitive relationship, the inhibitory effect of free ammonia molecules with bound water is enhanced, which leads to the maximum value of η moving toward the lower ammonia content.

3.2 Analysis of the $CaCO_3$ precipitation process

As can be seen from Fig. 3a, within the initial 420 s of the carbonation reaction, the pH drop rate showed an overall decrease, which was mainly attributed to the dissociation equilibrium shift of Asp from Asp^{2-} to Asp^- over the pH range of 10.15 to 9.97. More specifically, the dissociation of Asp upon variation in the solution pH is shown in Fig. 4. Thus, upon decreasing the solution pH, the unstable complex gradually releases Ca^{2+}, and the electron lone pair of the Asp^{2-} amino group can recombine with the protons (H^+) generated by the chemical absorption of CO_2, ultimately generating Asp^-. This leads to a slight reduction in the pH drop rate. Subsequently, owing to the accumulation of free Ca^{2+} and CO_3^{2-}, the reaction of $CaCO_3^0$ ion pair formation is enhanced, which further promotes CO_2 absorption.[29] As a result, the pH drop rate increased during the time interval from 420 to 700 s. In addition, a crystallization induction period of ~700 s was observed for the precipitation of $CaCO_3$, and this was due to the above variation in the pH drop rate. Notably, the dissociation equilibrium shift of Asp from Asp^{2-} to Asp^- significantly prolongs the induction time compared to the system where Asp is absent.[30] Furthermore, the conductivity was found to increase continuously during this period, and this was predominantly controlled by the chemical absorption of CO_2.[29] As shown in

Fig. 3b, the dissolved calcium content remained relatively unchanged during the initial 700 s of the reaction, during which the reaction solution became transparent, and only a very small amount of $CaCO_3$ precipitated. These results further confirm the existence of an extended induction period in the presence of Asp.

Beyond a reaction time of 700 s, the pH drop rate began to decrease and nucleation occurred. During a period of ~160 s, a large number of $CaCO_3$ nuclei were formed through the consumption of $CaCO_3^0$ ion pairs, and as a result, the rate of $CaCO_3^0$ ion pair formation decreased;[31] this was accompanied by a decrease in the pH drop rate. During the nucleation period,
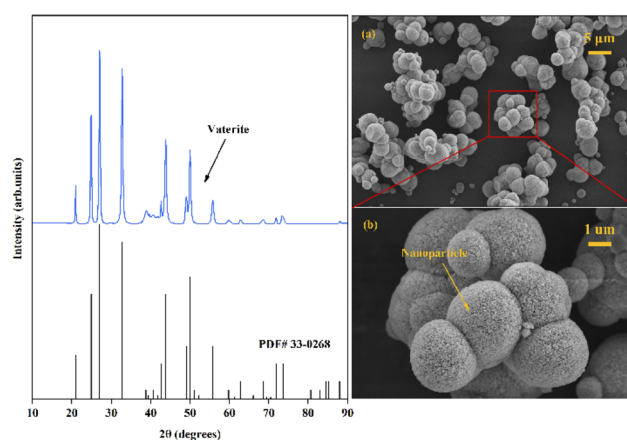

Fig. 5 XRD and SEM images ((a) scale bar 5 μm, (b) scale bar 1 μm) of the obtained $CaCO_3$ products.
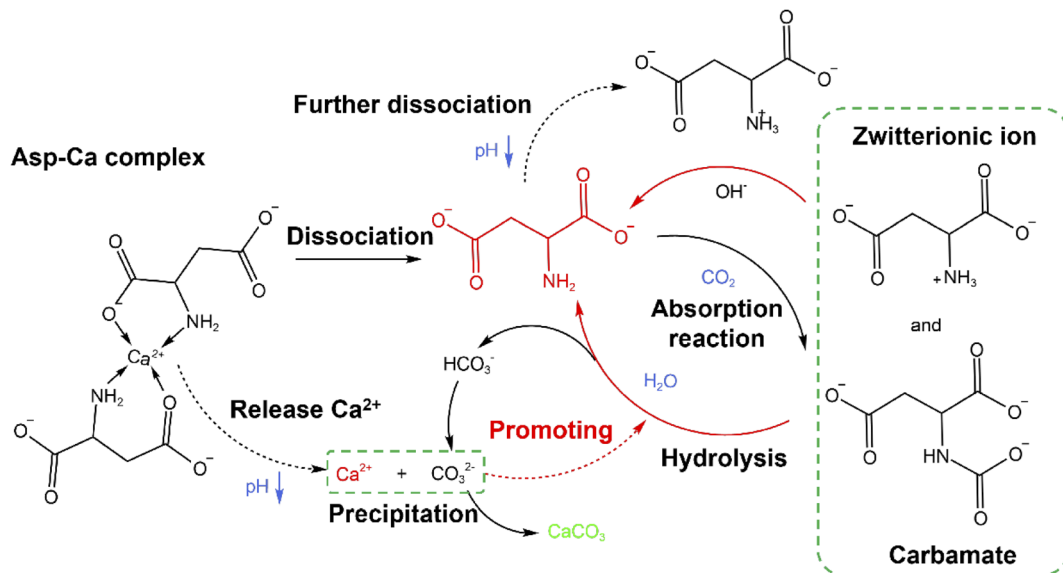
Fig. 6   The transformation mechanism of Asp during the carbonation reaction.

the conductivity of the reaction solution continued to increase since the total volume of the nucleus was relatively small and thus it contributed only weakly to the total ion content.[31]

Fig. 3a shows that the growth period began at 860 s, and this period can be divided into three stages. More specifically, area A (860–1400 s) corresponded to the rapid formation of $CaCO_3$, wherein the rate of CO_3^{2-} consumption was significantly higher than that of its formation. This led to a surge in the pH drop rate and a plunge in the conductivity. In addition, as shown in Fig. 3b, the dissolved calcium content decreased, and a large amount of $CaCO_3$ precipitated from the liquid phase. Subsequently, area B (1400–2100 s) corresponds to the stable crystal growth stage. During this stage, the solution conductivity and pH drop rate were close to their extreme points, and a dynamic balance between the consumption and formation rates of CO_3^{2-} was achieved. Finally, area C (2100–2500 s) represents the end of the growth period. Due to the minimal amount of dissolved calcium in the bulk solution at this stage (Fig. 3b), the CO_3^{2-} consumption rate decreased, and reached a value lower than its formation rate. As a result, the pH drop rate decreased significantly, while the conductivity jumped to >100 ms cm^{-1} at the end of this stage. In the final 500 s of the carbonation reaction, the variations in the pH drop rate and the conductivity were mainly controlled by the chemical absorption of CO_2. The amount of precipitated $CaCO_3$ reached a maximum level, and the termination of the carbonation reaction was considered achieved. Finally, the total carbonation efficiency was calculated as 54.2%.

Through examination of the XRD and SEM results presented in Fig. 5, the precipitated $CaCO_3$ products obtained in the presence of Asp were identified as spherical particles of the only vaterite phase. No characteristic peaks of calcite or aragonite phase were detected. The result was consistent with previous reported by Zheng et al.[32] who proposed a glycine-mediated leaching-mineralization cycle from coal fly ash. It seems that

a relatively high content of amino acid can help the formation of vaterite phase. According to Ostwald's step rule, the initial formation of the metastable vaterite is followed by its transformation into the more thermodynamically stable calcite.[33] However, during the growth period, organic additives such as Asp can adsorb onto the surface of the initially formed vaterite particles, which decreases the surface energy or creates a barrier to prevent the above phase transformation.[13] Moreover, the presence of Asp–Ca complex reduces the content of free Ca^{2+} in the bulk solution. As a new Ca source, the dissociation of the complex controls the release of Ca^{2+}, which influences the conversion of the precursor $CaCO_3^0$ ion pair, and therefore benefit the formation of vaterite.[13] Besides, the only vaterite phase can also obtain in excessive amount of ammonia (7 wt%
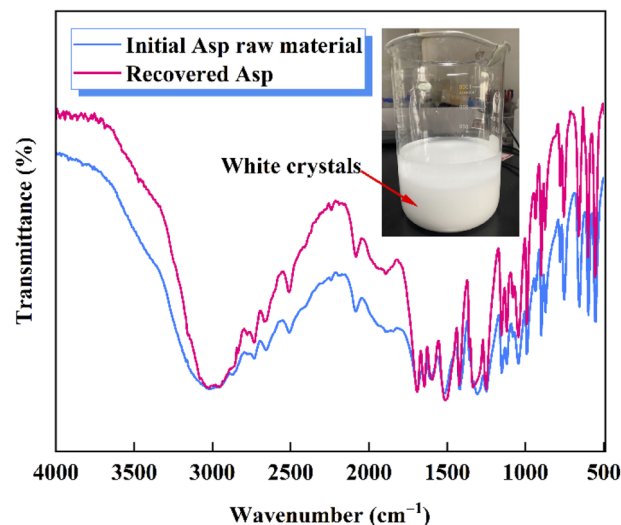

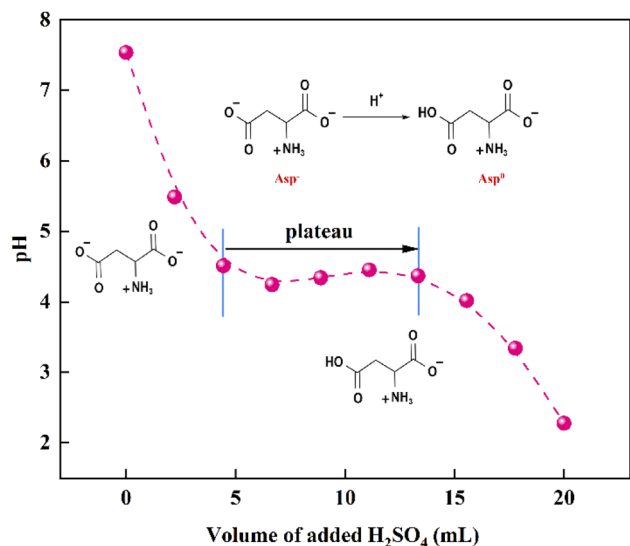Fig. 7   FTIR spectra of the initial Asp raw material and the recovered Asp.

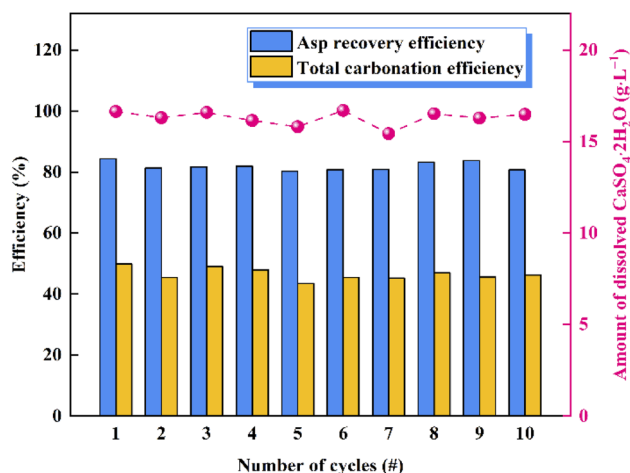**Fig. 8** Variation of the solution pH with the addition of H_2SO_4.

Fig. 9 Results of the 10 recycling experiments to confirm the reusability of Asp.

in the present study).[10] The SEM images show that the precipitated $CaCO_3$ microspheres are composed of aggregates of numerous nanoparticles, which can be accounted for by considering the primary–secondary particle theory.[34] In this

case, Asp controls the precipitation of $CaCO_3$ to produce stable spherical vaterite particles. Simultaneously, the Asp additive spontaneously undergoes absorption reaction and chemical regeneration, which are outlined in Fig. 6.

3.3 Recovery of Asp and determination of its cycling performance

Following the removal of $CaCO_3$, a 40 wt% H_2SO_4 solution was added to the evaporated filtrate to generate large quantities of white crystals (Fig. 7). As shown in the FTIR spectra, the recovered crystals were confirmed to be Asp. It should also be noted that upon the addition of H_2SO_4, the pH of the filtrate decreased, and so the dissociation equilibrium of Asp shifted toward the zwitterionic ion (Asp^0). As shown in Fig. 8, during the initial stage of H_2SO_4 addition (0–4.4 mL), the pH value decreased sharply from 7.5 to 4.5, at which point Asp was present mainly in the form of Asp^-. Subsequently, a plateau period was observed following the further addition of H_2SO_4 (4.4–13.3 mL), which leads to the combination of Asp^- with the abundant H^+ present in the bulk solution to generate Asp^0, and so the solution pH does not change to any great extent during this addition period. In addition, owing to the substantially lower solubility of Asp^0 under these conditions, high supersaturation was achieved, leading to the precipitation of large quantities of Asp from the filtrate during this plateau period. Upon the further addition of H_2SO_4 to a total volume of 20 mL, the pH value began to drop again until reaching the isoelectric point of Asp. As a result, the neutral Asp^0 became the main form of Asp present in the bulk solution. The Asp recovery efficiency was 89.2%.

To verify the cycling performance of Asp, 10 recycling experiments were carried out under identical experimental conditions after adding fresh Asp to the recovered crystals. More specifically, each cycle involved calcium leaching, the gas–liquid carbonation reaction, and Asp recovery. As shown in Fig. 9, the Asp recovery efficiency remained relatively stable at $81.9 \pm 1.4\%$, while the amount of dissolved $CaSO_4 \cdot 2H_2O$ and the total carbonation efficiency were 16.3 ± 0.4 g L^{-1} and $46.5 \pm 1.9\%$, respectively. Compared with other additives, as shown in Table 2, the leaching performance of Asp was similar to that of NH_4Cl, however, having higher carbonation efficiency which could be attributed to a higher liquid-to-solid ratio. Most importantly, the reaction efficiency of Asp kept an idea high

Table 2 Comparison of leaching, carbonation, and cycle performance in this study and previous studies

Additives	CaO^a (g)	η (g L^{-1})	γ (%)	λ (%)
NaCl[9]	5.92	9.0 ($c = 3$, LS $= 50$, $t = 30$)	47.6 ($Q = 80$, $t = 30$, $\theta = 60$)	40.3 (after 5 cycles)
CH$_3$COONH$_4$[10]	5.92	89.3 ($c = 6$, LS $= 10$, $t = 80$)	98.3 ($Q = 100$, $t = 30$, $\theta = 90$)	—
NH$_4$Cl[11]	5.92	18.7 ($c = 2$, LS $= 10$, $t = 60$)	20.2 ($Q = 50$, $t = 30$, $\theta = 60$)	42.6 (after 10 cycles)
Asp (this study)	4.87	19.5 ($c = 0.484$, LS $= 30$, $t = 30$)	54.2 ($Q = 500$, $t = 30$, $\theta = 50$)	90.5 (after 10 cycles)

^{a} The mass of raw material was calculated based on pure CaO. λ: the reaction efficiency ($\lambda = \frac{m_N}{m_0} \times 100\%$), where m_0 presents the mass of $CaCO_3$ when the additive was first used, and m_N denotes that under different cycle indices.[11] c: additive content, mol L^{-1}; LS: liquid-to-solid ratio, mL g^{-1}; t: temperature, °C; Q: CO_2 flow rate, mL min^{-1}; θ: carbonation reaction time, min.
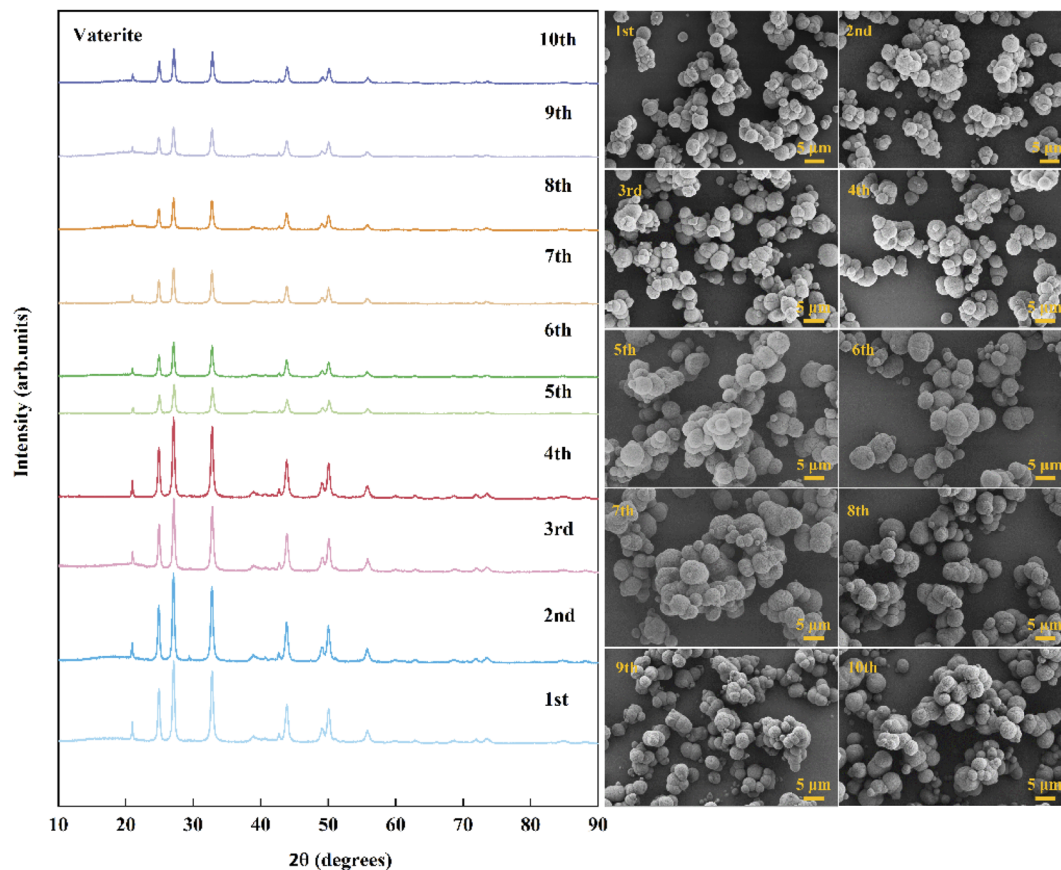
Fig. 10 XRD patterns and SEM images (scale bar 5 μm) of CaCO₃ recorded during the cycling.

level (90.5%) during the 10 recycling experiments, which was different from other inorganic additives. This indicates that the effective separation of Asp from the sulfate-rich carbonation filtrate was the key to its recycling. Finally, the precipitated CaCO₃ after each cycle was examined by XRD and SEM to observe any changes taking place during these experiments. As shown in Fig. 10, the spherical vaterite particles with diameters of 2–5 μm were recovered after each stage, and overall, the XRD and SEM results were consistent, thereby further confirming the reusability of Asp.

4. Conclusions

In conclusion, we proposed an indirect aqueous carbonation method of $CaSO_4 \cdot 2H_2O$ using aspartic acid (Asp) as recyclable additive. Our results indicated that the multiple roles of Asp were found as Ca^{2+} leaching agent, CO_2 absorbent, and CaCO₃ polymorph regulator in both the calcium leaching and subsequent gas–liquid carbonation reaction steps. More specifically, the dissolution capability of $CaSO_4 \cdot 2H_2O$ in aqueous ammonia was found to improve significantly through complexation between Asp and Ca^{2+}. Furthermore, the Asp^{2-} reacts with dissolved CO_2 and was then regenerated by means of the integrated CO_2 absorption and mineralisation (IAM) technique. The induction period during the carbonation reaction was extended owing to the dissociation equilibrium shift of Asp from Asp^{2-} to

Asp^-, which eventually controlled the conversion of the precursor $CaCO_3^0$ ion pair. As the final carbonation products, stable spherical vaterite particles were found. Based on the solubility characteristics of Asp upon variation in the pH, the regenerated Asp was successfully recovered from the sulfate-rich carbonation filtrate at its isoelectric point, with a recovery efficiency of >80% being achieved, and the reusability of the recycled Asp was further confirmed by recycling experiments. We believe that our study makes a significant contribution to the recycling and recovery of the leaching additives in the indirect aqueous carbonation process of $CaSO_4 \cdot 2H_2O$. Although the present study demonstrated the feasibility of Asp recovery and recycling, the recovery efficiency of Asp must be further improved to reduce the cost of this technology. Therefore, current work in our group is focusing on the thermodynamics and kinetics of Asp crystallisation from a solution containing a sulfate salt. Moreover, the recovery method of ammonia from the final filtrate after Asp separation and the comprehensive mechanism study of the carbonation reaction system in the presence of Asp are other important directions for future work.

Author contributions

Yuan Gong: conceptualization, formal analysis, investigation, methodology, writing – original draft, writing – review & editing.

Xuechen Zhu: formal analysis, validation, investigation, writing – review & editing. Zhuo Yang: validation, writing – review & editing. Xin Zhang: validation. Chunlei Li: conceptualization, supervision, project administration.

Conflicts of interest

There are no conflicts to declare.

Acknowledgements

References

1 S. P. Veetil and M. Hitch, *Int. J. Environ. Sci. Technol.*, 2020, **17**, 4359–4380.

2 A. Sanna, M. Uibu, G. Caramanna, R. Kuusik and M. M. Maroto-Valer, *Chem. Soc. Rev.*, 2014, **43**, 8049–8080.

3 A. M. Rashad, *J. Cleaner Prod.*, 2017, **166**, 732–743.

4 W. Liu, L. Teng, S. Rohani, Z. Qin, B. Zhao, C. C. Xu, S. Ren, Q. Liu and B. Liang, *Chem. Eng. J.*, 2021, **416**, 129093.

5 N. H. Koralegedara, P. X. Pinto, D. D. Dionysiou and S. R. Al-Abed, *J. Environ. Manage.*, 2019, **251**, 109572.

6 J. Zhou, Z. Sheng, T. Li, Z. Shu, Y. Chen and Y. Wang, *Ceram. Int.*, 2016, **42**, 7237–7245.

7 B. Wang, Z. Pan, H. Cheng, Z. Zhang and F. Cheng, *J. Cleaner Prod.*, 2021, **302**, 126930.

8 O. Rahmani, M. Tyrer and R. Junin, *RSC Adv.*, 2014, **4**, 45548–45557.

9 Q. Chen, W. Ding, H. Sun, T. Peng and G. Ma, *Energy*, 2020, **206**, 118148.

10 W. Ding, Q. Chen, H. Sun and T. Peng, *J. CO$_2$ Util.*, 2019, **34**, 507–515.

11 Q. Chen, W. Ding, H. Sun, T. Peng and G. Ma, *ACS Sustainable Chem. Eng.*, 2020, **8**, 11649–11657.

12 B. Yang, M. Yang, B. Wang, X. Fang and Q. Wan, *Mater. Res. Express*, 2019, **6**, 45042.

13 J. Luo, F. Kong and X. Ma, *Cryst. Growth Des.*, 2016, **16**, 728–736.

14 X. Yu, *Handbook of MSG industry*, China Light Industry Press Ltd, Beijing, 2009.

15 B. Bonfils, C. Julcour-Lebigue, F. Guyot, F. Bodénan, P. Chiquet and F. Bourgeois, *Int. J. Greenhouse Gas Control*, 2012, **9**, 334–346.

16 R. M. Santos, Y. W. Chiang, J. Elsen and T. Van Gerven, *Hydrometallurgy*, 2014, **147–148**, 90–94.

17 K. Song, W. Kim, S. Park, J.-H. Bang, C. W. Jeon and J.-W. Ahn, *Chem. Eng. J.*, 2016, **301**, 51–57.

18 X. Liu, B. Wang, Z. Zhang, Z. Pan, H. Cheng and F. Cheng, *Environ. Chem. Lett.*, 2022, **20**, 2261–2269.

19 Y. Li, X. Duan, W. Song, L. Ma and J. Jow, *Chem. Eng. J.*, 2021, **405**, 126938.

20 V. Sang Sefidi and P. Luis, *Ind. Eng. Chem. Res.*, 2019, **58**, 20181–20194.

21 M. Liu and G. Gadikota, *Fuel*, 2020, **275**, 117887.

22 L. Ji, H. Yu, K. Li, B. Yu, M. Grigore, Q. Yang, X. Wang, Z. Chen, M. Zeng and S. Zhao, *Appl. Energy*, 2018, **225**, 356–366.

23 Z. Yan, Y. Wang, H. Yue, C. Liu, S. Zhong, K. Ma, W. Liao, S. Tang and B. Liang, *ACS Sustainable Chem. Eng.*, 2021, **9**, 8238–8248.

24 L. Ji, X. Zheng, S. Yan and Q. He, *CN. Pat.*, 113443628A, 2021.

25 O. Rahmani, *J. CO$_2$ Util.*, 2020, **35**, 265–271.

26 I. Hammas, K. Horchani-Naifer and M. Férid, *Int. J. Miner. Process.*, 2013, **123**, 87–93.

27 J. Ge, J. Zhu, S. Xia and S. Liu, *CIESC J.*, 2018, **69**, 2829–2837.

28 L. Wu, J. Li, J. Zhu, Y. Gong and J. Ge, *CIESC J.*, 2020, **71**, 3575–3584.

29 M. Vučak, J. Perić, A. Žmikić and M. N. Pons, *Chem. Eng. J.*, 2002, **87**, 171–179.

30 K. Song, Y.-N. Jang, W. Kim, M. G. Lee, D. Shin, J.-H. Bang, C. W. Jeon and S. C. Chae, *Chem. Eng. J.*, 2012, **213**, 251–258.

31 Y. Gong, L. Wu, J. Li and J. Zhu, *J. Cryst. Growth*, 2019, **522**, 128–138.

32 X. Zheng, J. Liu, Y. Wei, K. Li, H. Yu, X. Wang, L. Ji and S. Yan, *Chem. Eng. J.*, 2022, **440**, 135900.

33 C. C. Yec and H. C. Zeng, *J. Mater. Chem. A*, 2014, **2**, 4843–4851.

34 Y. Lai, L. Chen, W. Bao, Y. Ren, Y. Gao, Y. Yin and Y. Zhao, *Cryst. Growth Des.*, 2015, **15**, 1194–1200.